Cross-Species Analysis of the Glycolytic Pathway by Comparison of Molecular Interaction Fields

Matthias Stein, Razif R. Gabdoulline, Rebecca C. Wade

Supplementary Information

Table of Contents

1. Choice of protein sequences and structural templates

Step 01 Template Used 1V4S
Q91753_XENLA
Q8AYP7_CHICK
HXK2_DROME
Q5TW28_ANOGA
Q6NX09_BRARE
HXK4_HUMAN
HXK4_MOUSE
HXK2_ARATH
HXK4_RAT
Q6Z398_ORYSA
Q5RC71_PONPY

Step 02 Template Used 1HOX
G6PI_PONPY
G6PI_DROME
Q6GP33_XENLA
Q5ZMU3_CHICK
Q8QFU1_BRARE
G6PI_MOUSE
Q6P6V0_RAT
G6PIA_ORYSA
G6PI_HUMAN
Q7PVA2_ANOGA
G6PI_ARATH

Step 03 Template Used 4PFK
K6PL_HUMAN
Q5R7V5_PONPY
K6PL_RAT
K6PL_MOUSE
Q90YA3_CHICK
Q6DD69_XENLA
Q66HV8_BRARE
K6PF_DROME
Q7QJT0_ANOGA
Q5SNH5_ORYSA
Q9M0F9_ARATH

Step 04 Template Used 1FDJ
ALDOB_CHICK
ALDOB_DANRE
ALDOB_HUMAN
ALDOB_MOUSE
ALDOB_PONPY
ALDOB_RAT
ALF_ARATH
ALF_DROME
ALF_ORYSJ
Q5XHC6_XENLA
Q7PGI9_ANOGA

Step 05 Template Used 1R2R
Q7PXW5_ANOGA_xp_321467.2
TPIS_DROME
Q90XG0_DANRE
TPIS_CHICK
Q7ZWN5_XENLA
TPIS_RAT
Q5R928_PONPY

TPIS_HUMAN
TPIS_MOUSE
TPIS_ORYSJ
TPIS_ARATH

Step 06 Template Used 1NQO
G3PB_ARATH
G3P_MOUSE
G3P_CHICK
Q7Q1U8_ANOGA
G3P2_DROME
Q5RAB4_PONPY
G3P2_HUMAN
G3P_XENLA
Q6NYM9_BRARE
G3PC_ORYSA

Step 07 Template Used 1HDI
PGK1_HUMAN
PGK1_PONPY
PGK1_MOUSE
PGK1_RAT
PGK_CHICK
Q7ZV29_BRARE
PGK_XENLA
PGK_ANOGA
PGK_DROME
Q655T1_ORYSA
PGKH_ARATH

Step 08 Template Used 1YFK
PGAM1_HUMAN
PGAM1_RAT
PGAM1_MOUSE
PGAM1_PONPY
Q6TNR9_BRARE
PGAM1_CHICK
Q6AZP8_XENLA
Q9VAN7_DROME
Q7PXI5_ANOGA
Q6Z8J0_ORYSA
Q9LM13_ARATH

Step 09 Template Used 2ONE
ENO_DROME
Q7Q3D8_ANOGA
Q6TH14_BRARE
ENOB_HUMAN
ENOA_CHICK
ENOB_MOUSE
Q5R6Y1_PONPY
ENOB_RAT
ENO_XENLA
ENO_ORYSA
ENO_ARATH

Step 10 Template Used 1LIU
KPYK_DROME
Q7PPE7_ANOGA
KPYR_HUMAN
KPYR_MOUSE
KPYR_RAT
KPYK_CHICK

KPYM_PONPY
KPYK_XENLA
Q7ZVT2_BRARE
Q7XKB5_ORYSA
KPYC_ARATH

2. Evaluation of the choice of PDB template on the similarity of electrostatic potentials

The PGI from rabbit (PDB entry 1HOX) and the protein structure from human autocrine motility factor (PDB entry 1JIQ) were used as the structural templates (the RMSD between the two crystal structures is 0.63 Å for backbone atoms and 0.91 Å for all atoms; using SuperPose1.0 (Maiti R, van Domselaar GH, Zhang H., Wishart DS (2004) SuperPose: a simple server for sophisticated structural superposition. Nucl. Acids Res. **32**: W590-W594)..We repeated the multiple sequence alignment of the eleven model PGI sequences using ClustalW, used the two PDB entries as the template structures, calculated the electrostatic potentials with UHBD and ranked the PGI enzymes according to their similarity to the human enzyme (Table SI).

The percentage sequence identity between the modelled sequences and the templates is high for both PDB templates (see Table SI). The overall rather high sequence identity for PGIs enables the generation of protein structural models with confidence. The lowest sequence identity to the human enzyme is found for the PGI from rice (47% and 46%, respectively). The Hodgkin similarity indices vary very little whether using the PGI from rabbit or human as protein templates. The largest difference in similarity indices is found for the PGI from rice which varies from 0.34 (1HOX template) to 0.46 (1JIQ template) (see Table SI). This value of about 0.1 may thus be considered as an estimate of the uncertainty in Hodgkin SIs when discussing the relation between two proteins in terms of their electrostatic potentials.

The PGI from mosquito (*Anopheles gambiae*) is less affected by the choice of protein template structure. The electrostatic potential shows no correlation with that of the human enzyme when using either the rabbit or the human protein as a template structure (Hodgkin SI 0.07 and 0.04, respectively).

Table SI: Comparison of the calculated Hodgkin similarity indices of the electrostatic potentials for glucose 6-phosphate isomerases (PGI) using two different template structures: The PGI from *Oryctolagus cuniculus* (rabbit; PDB entry 1HOX) and *Homo sapiens* (PDB entry 1JIQ).

PDB Template 1HOX (Rabbit)	PDB Template 1JIQ (Human)

SwissProt ID	%SeqID	Hodgkin SI	%SeqID	Hodgkin SI
G6PI_HUMAN	93.0	1.00	100.0	1.00
G6PI_PONPY	92.4	0.95	98.9	0.97
G6PI_MOUSE	89.7	0.84	89.2	0.85
Q6P6V0_RAT	89.2	0.78	88.5	0.75
Q6GP33_XENLA	80.3	0.69	79.7	0.69
Q5ZMU3_CHICK	82.6	0.67	82.2	0.65
Q8QFU1_BRARE	77.8	0.60	78.9	0.60
G6PIA_ORYSA	47.4	0.34	46.0	0.46
G6PI_ARATH	48.3	0.27	47.8	0.39
G6PI_DROME	68.7	0.23	68.3	0.25
Q7PVA2_ANOGA	68.4	0.07	68.4	0.04

3. Visualisation of distance matrices of electrostatic potentials

Step	Entire Protein	Active Site
01	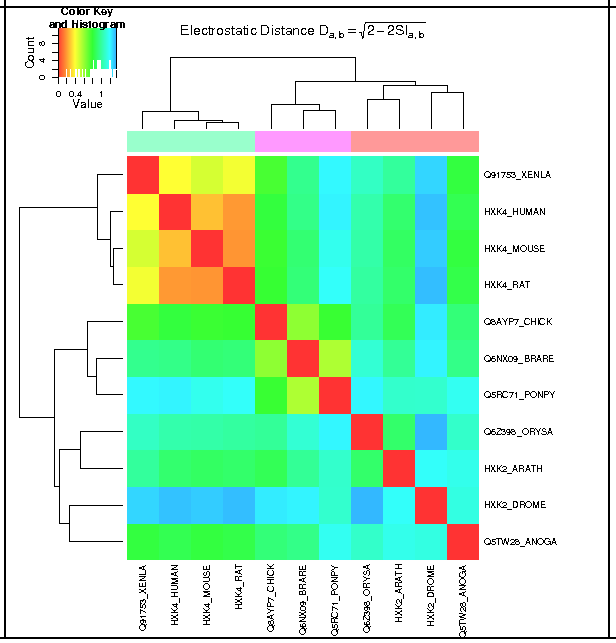	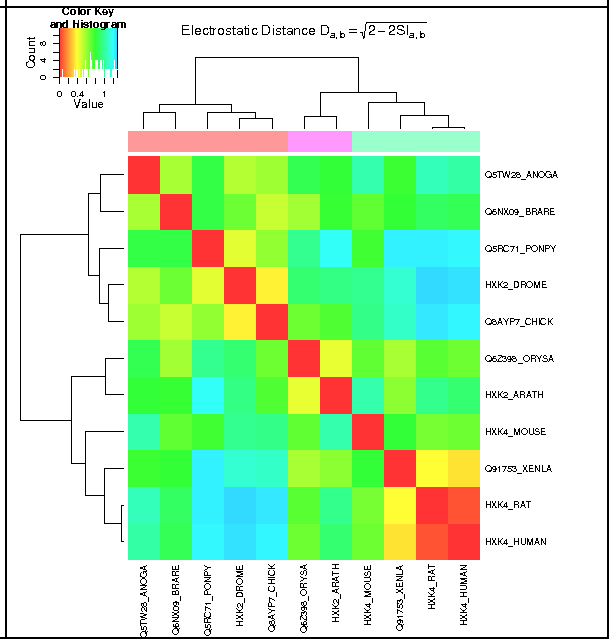

02

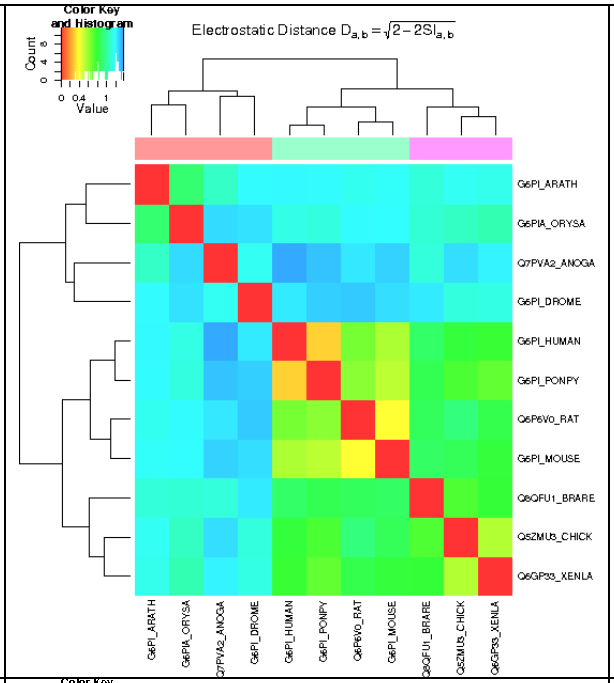
Color Key and Histogram
Count
Value
Electrostatic Distance $D_{a,b} = \sqrt{2 - 2S|_{a,b}}$
Q6PI_ARATH
Q6PIA_ORYSA
Q7PVA2_ANOGA
Q6PI_DROME
Q6PI_HUMAN
Q6PI_PONPY
Q6P6V0_RAT
Q6PI_MOUSE
Q8QFU1_BRARE
Q5ZMU5_CHICK
Q6GP33_XENLA

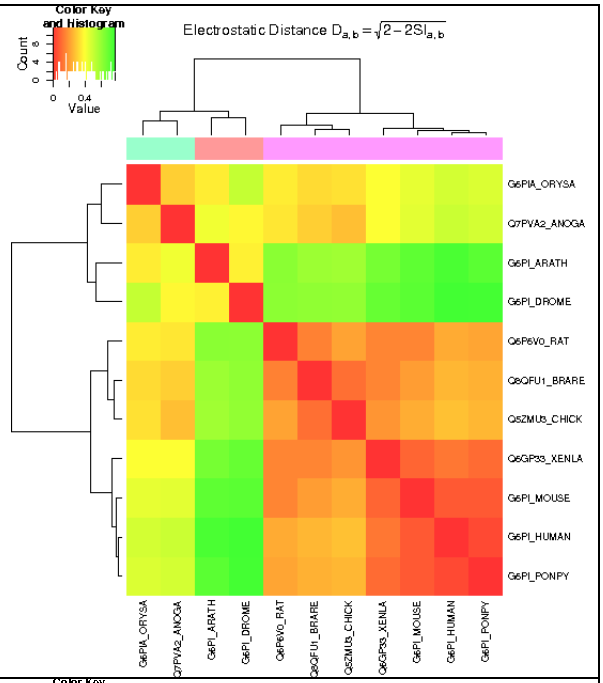
Color Key and Histogram
Count
Value
Electrostatic Distance $D_{a,b} = \sqrt{2 - 2S|_{a,b}}$
Q6PIA_ORYSA
Q7PVA2_ANOGA
Q6PI_ARATH
Q6PI_DROME
Q6P6V0_RAT
Q8QFU1_BRARE
Q5ZMU5_CHICK
Q6GP33_XENLA
Q6PI_MOUSE
Q6PI_HUMAN
Q6PI_PONPY

03

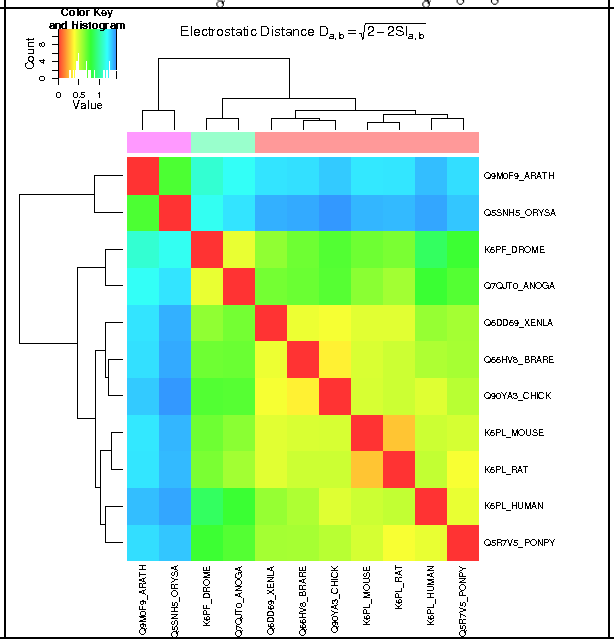
Color Key and Histogram
Count
Value
Electrostatic Distance $D_{a,b} = \sqrt{2 - 2S|_{a,b}}$
Q9M0F9_ARATH
Q5SNH5_ORYSA
K6PF_DROME
Q7QJT0_ANOGA
Q6DD69_XENLA
Q66HV8_BRARE
Q90YA3_CHICK
K6PL_MOUSE
K6PL_RAT
K6PL_HUMAN
Q5R7V5_PONPY

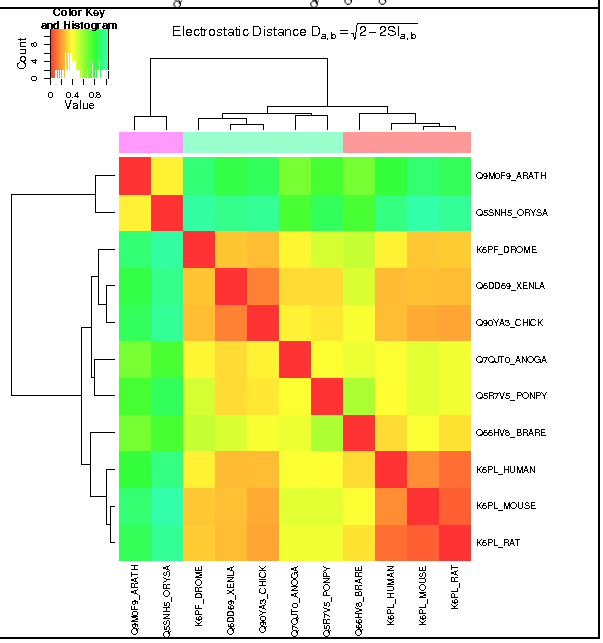
Color Key and Histogram
Count
Value
Electrostatic Distance $D_{a,b} = \sqrt{2 - 2S|_{a,b}}$
Q9M0F9_ARATH
Q5SNH5_ORYSA
K6PF_DROME
Q6DD69_XENLA
Q90YA3_CHICK
Q7QJT0_ANOGA
Q5R7V5_PONPY
Q66HV8_BRARE
K6PL_HUMAN
K6PL_MOUSE
K6PL_RAT

04

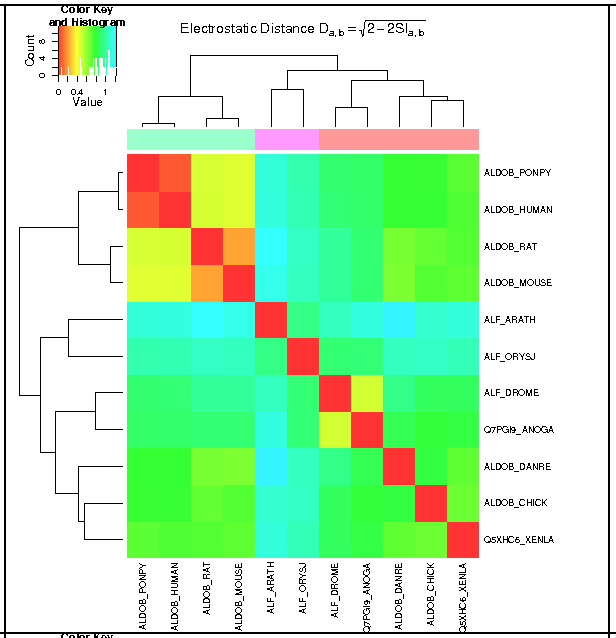
Color Key and Histogram
Count
Value
Electrostatic Distance $D_{a,b} = \sqrt{2 - 2S|_{a,b}}$
ALDOB_PONPY
ALDOB_HUMAN
ALDOB_RAT
ALDOB_MOUSE
ALF_ARATH
ALF_ORYSJ
ALF_DROME
Q7PGI9_ANOGA
ALDOB_DANRE
ALDOB_CHICK
Q5XHC6_XENLA

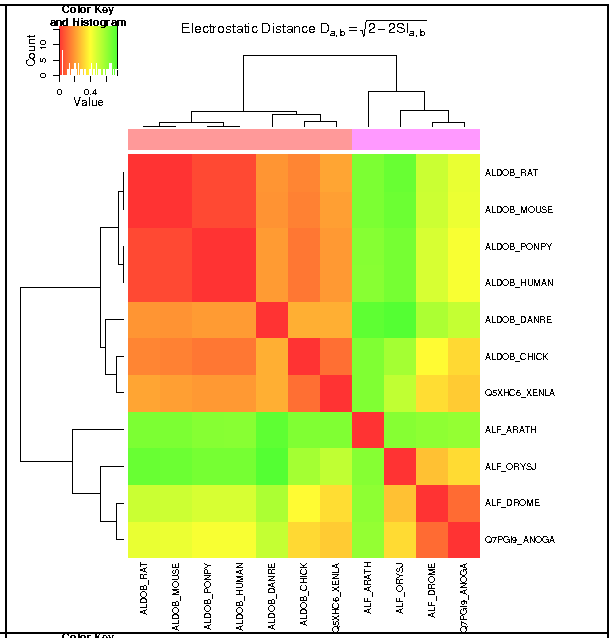
Color Key and Histogram
Count
Value
Electrostatic Distance $D_{a,b} = \sqrt{2 - 2S|_{a,b}}$
ALDOB_RAT
ALDOB_MOUSE
ALDOB_PONPY
ALDOB_HUMAN
ALDOB_DANRE
ALDOB_CHICK
Q5XHC6_XENLA
ALF_ARATH
ALF_ORYSJ
ALF_DROME
Q7PGI9_ANOGA

05

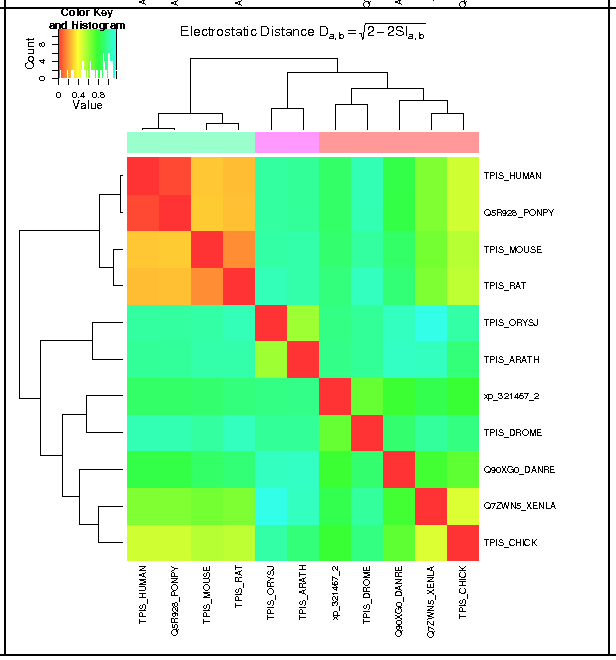
Color Key and Histogram
Count
Value
Electrostatic Distance $D_{a,b} = \sqrt{2 - 2S|_{a,b}}$
TPIS_HUMAN
Q5R926_PONPY
TPIS_MOUSE
TPIS_RAT
TPIS_ORYSJ
TPIS_ARATH
xp_321457_2
TPIS_DROME
Q90XG0_DANRE
Q7ZWN5_XENLA
TPIS_CHICK

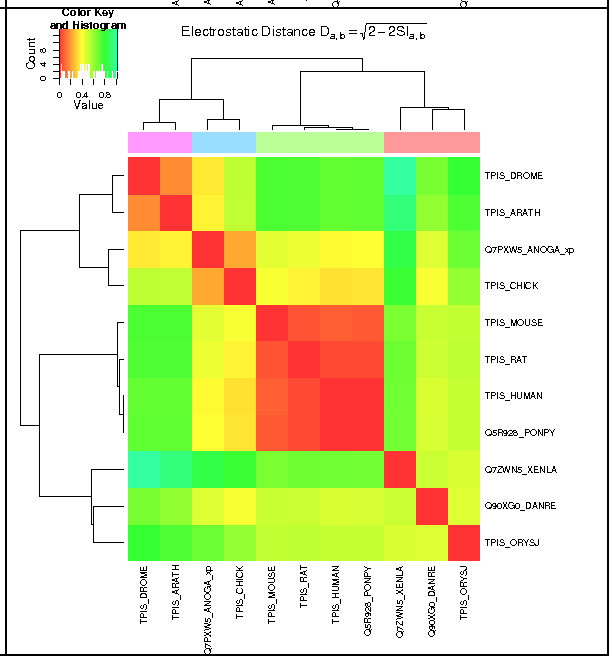
Color Key and Histogram
Count
Value
Electrostatic Distance $D_{a,b} = \sqrt{2 - 2S|_{a,b}}$
TPIS_DROME
TPIS_ARATH
Q7PXW5_ANOGA_xp
TPIS_CHICK
TPIS_MOUSE
TPIS_RAT
TPIS_HUMAN
Q5R926_PONPY
Q7ZWN5_XENLA
Q90XG0_DANRE
TPIS_ORYSJ

06

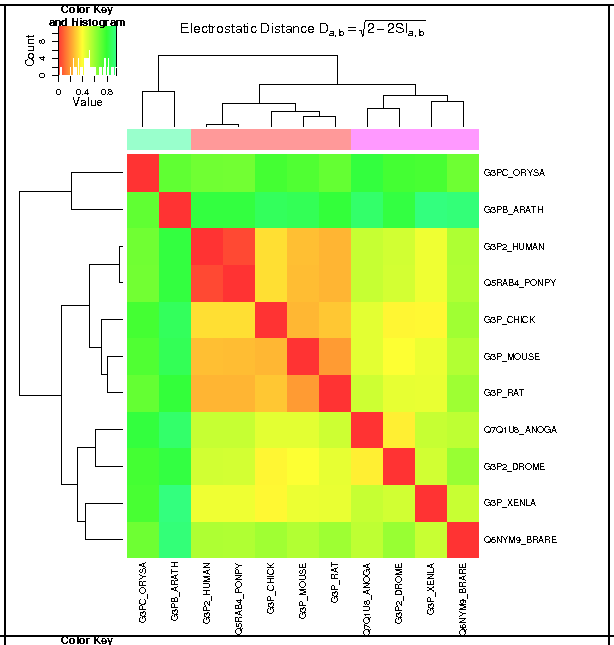
Color Key and Histogram
Count
Value
Electrostatic Distance $D_{a,b} = \sqrt{2 - 2S|_{a,b}}$
G3PC_ORYSA
G3PB_ARATH
G3P2_HUMAN
Q5RAB4_PONPY
G3P_CHICK
G3P_MOUSE
G3P_RAT
Q7Q1U8_ANOGA
G3P2_DROME
G3P_XENLA
Q6NYM9_BRARE

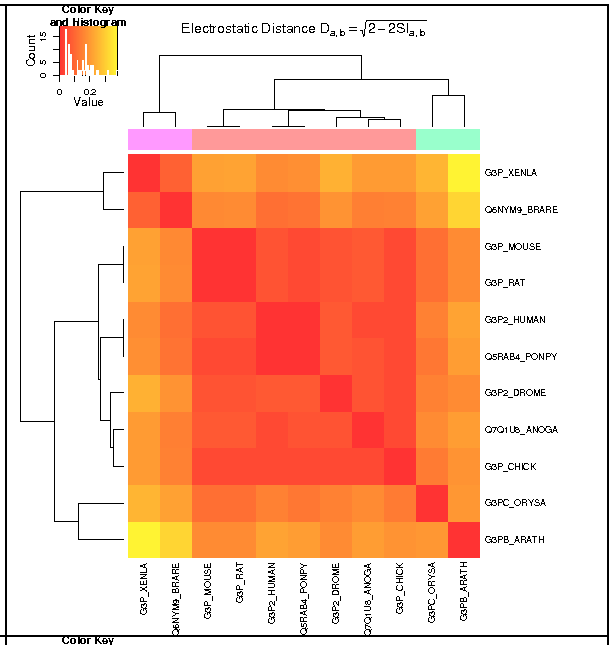
Color Key and Histogram
Count
Value
Electrostatic Distance $D_{a,b} = \sqrt{2 - 2S|_{a,b}}$
G3P_XENLA
Q6NYM9_BRARE
G3P_MOUSE
G3P_RAT
G3P2_HUMAN
Q5RAB4_PONPY
G3P2_DROME
Q7Q1U8_ANOGA
G3P_CHICK
G3PC_ORYSA
G3PB_ARATH

07

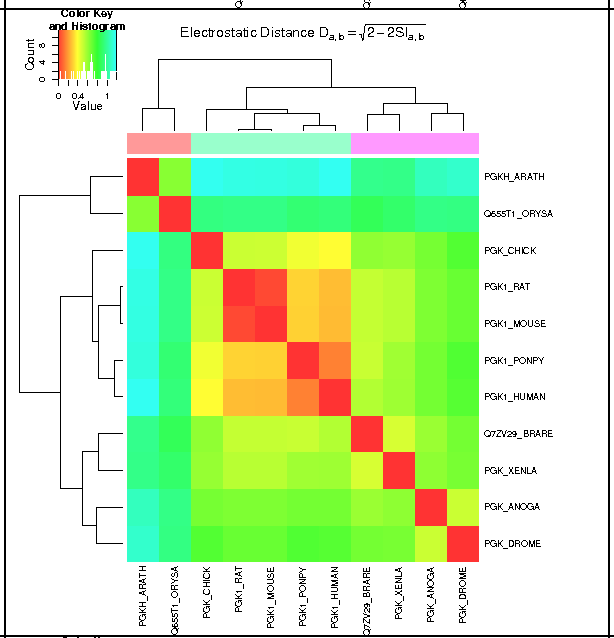
Color Key and Histogram
Count
Value
Electrostatic Distance $D_{a,b} = \sqrt{2 - 2S|_{a,b}}$
PGKH_ARATH
Q655T1_ORYSA
PGK_CHICK
PGK1_RAT
PGK1_MOUSE
PGK1_PONPY
PGK1_HUMAN
Q7ZV29_BRARE
PGK_XENLA
PGK_ANOGA
PGK_DROME

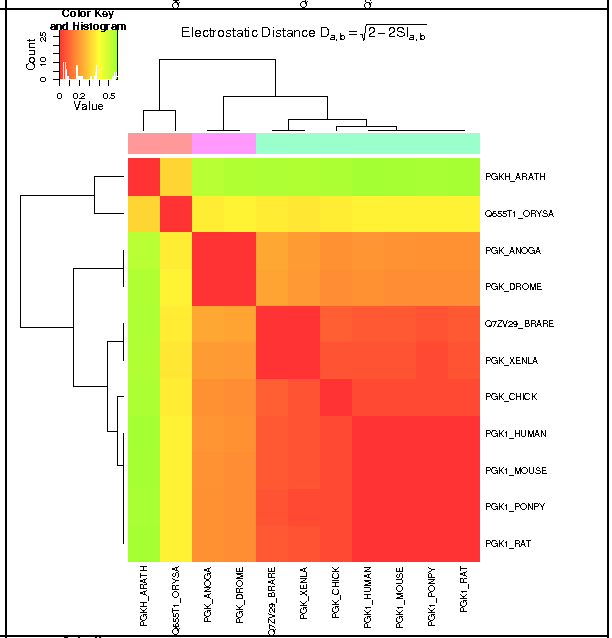
Color Key and Histogram
Count
Value
Electrostatic Distance $D_{a,b} = \sqrt{2 - 2S|_{a,b}}$
PGKH_ARATH
Q655T1_ORYSA
PGK_ANOGA
PGK_DROME
Q7ZV29_BRARE
PGK_XENLA
PGK_CHICK
PGK1_HUMAN
PGK1_MOUSE
PGK1_PONPY
PGK1_RAT

08

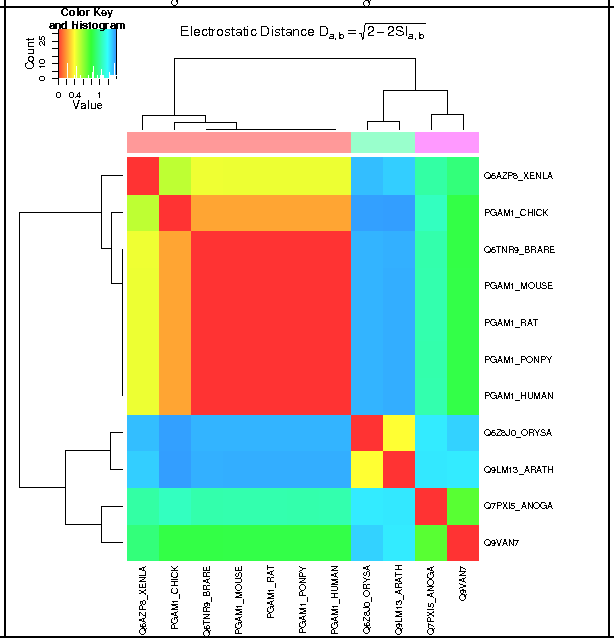
Color Key and Histogram
Count
Value
Electrostatic Distance $D_{a,b} = \sqrt{2 - 2S|_{a,b}}$
Q6AZP8_XENLA
PGAM1_CHICK
Q6TNR9_BRARE
PGAM1_MOUSE
PGAM1_RAT
PGAM1_PONPY
PGAM1_HUMAN
Q6ZBJ0_ORYSA
Q9LM13_ARATH
Q7PXI5_ANOGA
Q9VAN7

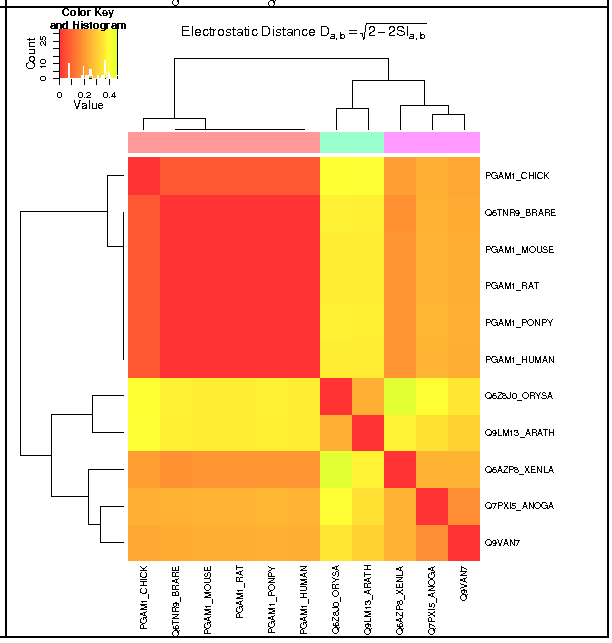
Color Key and Histogram
Count
Value
Electrostatic Distance $D_{a,b} = \sqrt{2 - 2S|_{a,b}}$
PGAM1_CHICK
Q6TNR9_BRARE
PGAM1_MOUSE
PGAM1_RAT
PGAM1_PONPY
PGAM1_HUMAN
Q6ZBJ0_ORYSA
Q9LM13_ARATH
Q6AZP8_XENLA
Q7PXI5_ANOGA
Q9VAN7

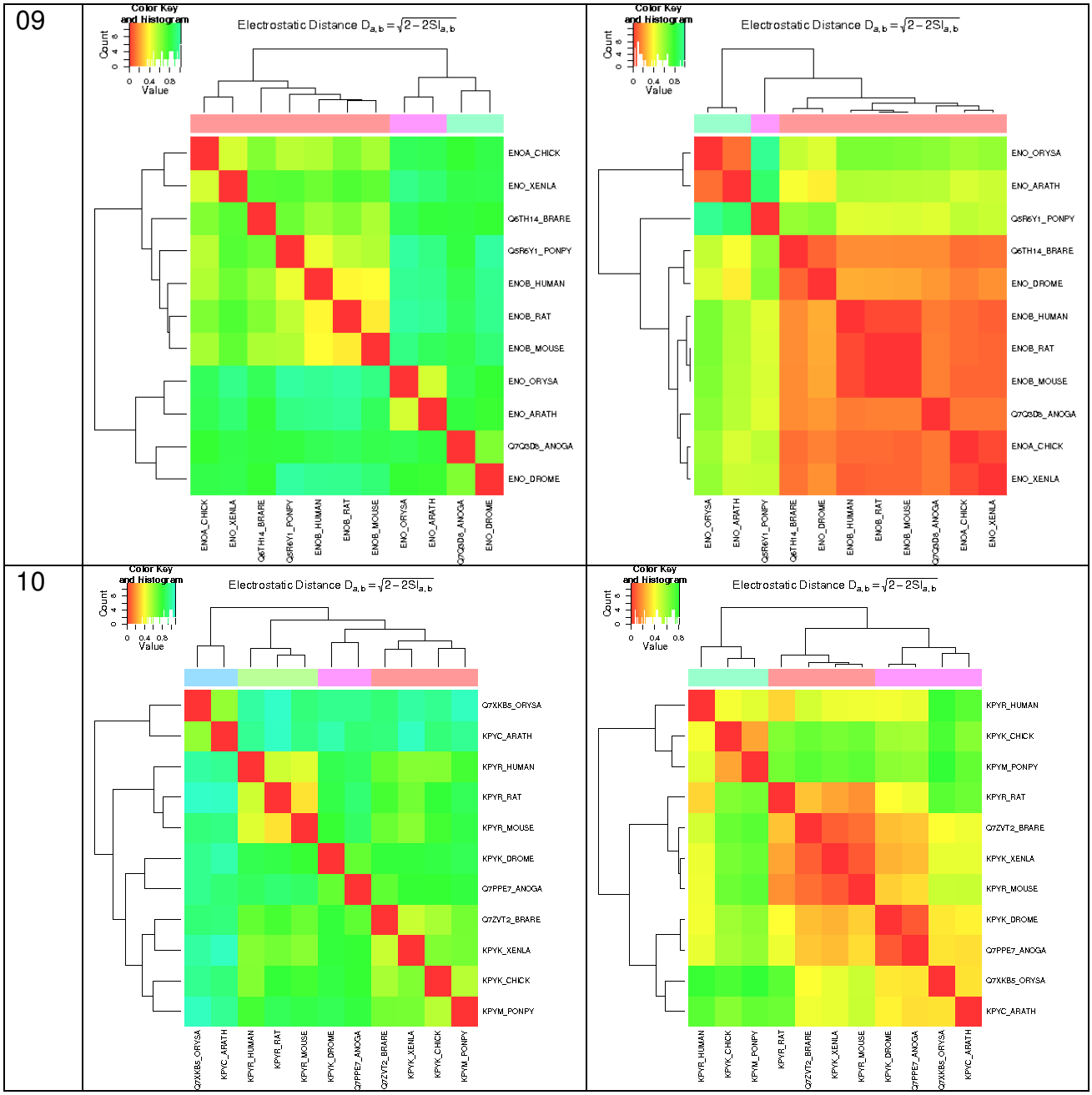

4. Discussion of means to compare electrostatic potentials

The Hodgkin similarity index measures relative similarities of two three-dimensional fields. The scalar product of fields (2*a*b) is divided by the sum of squares (a^2+b^2) and thus one obtains a **relative** measure of the similarities of molecular interaction fields. For example for enolases (step 09) one observes rather large electrostatic potential differences between the model species (Figure 9C), but Hodgkin similarity indices close to unity (Figure 9B) because of the large (and negative) magnitude of the electrostatic potential around the active site

(Figure 9D). The same argument holds for PGIs (step 02) which exhibit a large (and positive) electrostatic potential around the active site (Figure 9D) and large electrostatic potential differences between the species (Figure 9C) but Hodgkin similarity indices which are between 0.7 and 1.0 (Figure 9B). For triosephosphate isomerases (step 05), the electrostatic potential at the active site is very small in magnitude (Figure 9D). Thus relatively small differences in electrostatic potentials around the active site between the species (Figure 9C) lead to larger differences in Hodgkin similarity indices (Figure 9B) for that region. An **absolute** electrostatic potential difference (Figure 9C) gives a more quantitative means of comparing enzyme kinetic parameters between different species. It is the absolute difference in electrostatic potentials that is, for example important for stabilizing the transition state, and can therefore be related to species-to-species variations in kinetic parameters.